

# Modern Valence-Bond Descriptions of Polycyclic Fused Aromatic Compounds Involving Cyclopropenyl Rings

Peter B. Karadakov<sup>a,\*</sup> and David L. Cooper<sup>b,\*</sup>

<sup>a</sup>*Department of Chemistry, University of York, Heslington, York, YO10 5DD, U.K.*

<sup>b</sup>*Department of Chemistry, University of Liverpool, Liverpool L69 7ZD, U.K. \**

## Abstract

The feasibilities and electronic structures of five ten- $\pi$ -electron fused conjugated molecules involving cyclopropenyl rings are explored using second-order Møller-Plesset perturbation theory (MP2), spin-coupled (SC) and complete-active-space self-consistent-field (CASSCF) wavefunctions, in the cc-pVTZ basis. All five fused conjugated molecules are predicted to have rigid planar ground state geometries of  $C_{2v}$  or  $D_{2h}$  symmetry and large dipole moments (if not of  $D_{2h}$  symmetry). The compact ground state SC(10) wavefunctions with ten active orbitals for these molecules are found to be of comparable quality to the respective CASSCF(10,10) constructions, but much easier to interpret. The analyses of the ground state SC(10) wavefunctions for all five fused conjugated molecules reveal resonance patterns which indicate that all of these molecules are aromatic in their electronic ground states; on the other hand, the SC(10) approximations to the first singlet electronic excited states are found to exhibit “antiresonance” which suggests that each of the five molecules switches from aromatic to antiaromatic upon vertical excitation from the ground state to its first singlet excited state. Ring strain prevents the formation of a fused structure involving three cyclopropenyl rings and a cycloheptatrienyl ring; the alternative stable dehydro compound which resembles *m*-benzynes is shown, using a SC(12) wavefunction, to involve a weak  $\sigma$  bond between the dehydro centres.

**Keywords:** Spin-coupled theory, Modern valence-bond theory, Aromaticity, Antiaromaticity, Fused conjugated systems, Excited state aromaticity

## 1 Introduction

The best-known example of a bicyclic aromatic system containing two odd-membered rings is of course azulene, an isomer of naphthalene, which can be viewed as the result of the fusion of two aromatic ions, namely a cyclopentadienyl anion and a cycloheptatrienyl (tropylium) cation, each of which has six  $\pi$  electrons and so follows Hückel’s  $4n + 2$  rule. This notional process formally gives rise to a charge separation that is often used to explain the large dipole moment of azulene. The properties and reactivity of azulene indicate that it is less aromatic than naphthalene.

Spin-coupled (SC) theory, a modern valence-bond (VB) approach which usually provides a close approximation to a complete-active-space self-consistent field (CASSCF) wavefunction, but can be interpreted in terms of a small number of VB resonance structures involving non-orthogonal orbitals [1,2]

---

\*Corresponding authors.

*E-mail addresses:* peter.karadakov@york.ac.uk (P.B. Karadakov), dlc@liverpool.ac.uk (D.L. Cooper).

has previously been used to obtain a detailed description of the  $\pi$ -electron system of azulene [3]. The  $\pi$ -space SC wavefunction for azulene was based on a single product of ten singly-occupied non-orthogonal active (or spin-coupled) orbitals, engaged within a spin-coupling pattern that included contributions from all 42 unique ten-electron singlet spin eigenfunctions. The optimal SC orbitals turned out to be atom-centred and well-localized, similar in shape to  $C(2p_\pi)$  atomic orbitals but with small symmetrical protrusions towards neighbouring carbon atoms. The optimal spin-coupling pattern, expressed in terms of Rumer spin functions [4], was found to be dominated by two equivalent Kekulé-like structures, as chemical intuition would suggest. While all of the numerical characteristics of the SC wavefunction for azulene [3] indicate that it is of a very reasonable quality, this wavefunction does not explicitly include any of the classical VB ionic resonance structures which have been used by organic chemists to explain the dipole moment of azulene. This suggests that the importance of such ionic structures is sufficiently low that they can be fully “absorbed” via the protrusions of the atom-centred SC orbitals towards neighbouring atoms. This makes the SC wavefunction for azulene more compact, as well as easier to visualize and interpret.

Naphthalene has another isomer, which can notionally be constructed by fusing a cyclopropenium cation and a cyclononatetraenyl anion, aromatic rings with two and ten  $\pi$  electrons, respectively. This isomer of naphthalene, bicyclo[7.1.0]deca-1,3,5,7,9-pentaene (see structure **1** in Figure 1) which, using a terminology suggested by Sondheimer [6], can be called [3]annuleno[9]annulene, has not yet been synthesized, but it has been the subject of several theoretical studies, starting with a semiempirical investigation by Toyota and Nakajima [7] which aimed to establish whether **1** could experience a second-order Jahn-Teller effect, reducing the symmetry of the ground-state geometry from  $C_{2v}$  to  $C_s$ . Those authors concluded that **1** is stable with respect to a distortion of this type; their optimized geometry for **1** exhibits remarkable bond equalization along the periphery of the carbon framework. Not unexpectedly, a Hückel molecular orbital (HMO) calculation on **1** [8] showed that it has positive resonance energy per electron (REPE), which is another argument in favour of aromaticity. The aromaticity of **1** has been confirmed in a study of ring current patterns in annelated bicyclic polyenes at the Hartree-Fock (HF) level [9], and in a very recent density functional theory (DFT) investigation of the fused-to-single ring evolution of structures with ten  $\pi$  electrons [10].

In this paper we use second-order Møller-Plesset perturbation theory (MP2), as well as SC and CASSCF wavefunctions, to examine the feasibilities and the electronic structures of various ten- $\pi$ -electron bi-, tri- and tetracyclic fused conjugated molecules involving cyclopropenyl rings, starting with **1** (see Figure 1). Out of the remaining compounds, only **2** (tricyclo[7.1.0.0<sup>4,6</sup>]deca-1,3,5,7,9-pentaene) has been studied before, by Toyota [11], in a continuation of the research reported in [7]. The semiempirical results obtained by Toyota suggest that, similarly to **1**, the ground state geometry of **2** is stable with respect to a second-order Jahn-Teller effect that would reduce the symmetry, in this case from  $D_{2h}$  to  $C_{2h}$ , and that the optimized geometry for **2** is also characterized by significant bond equalization along the periphery of the carbon framework.

## 2 Methodology, Results and Discussion

The gas-phase ground state geometries of azulene and of compounds **1–5** (see Figure 1) were optimized using second-order Møller-Plesset perturbation theory with the cc-pVTZ basis, including all orbitals in the correlation treatment [MP2(Full)/cc-pVTZ]. Each optimized geometry was confirmed as a local

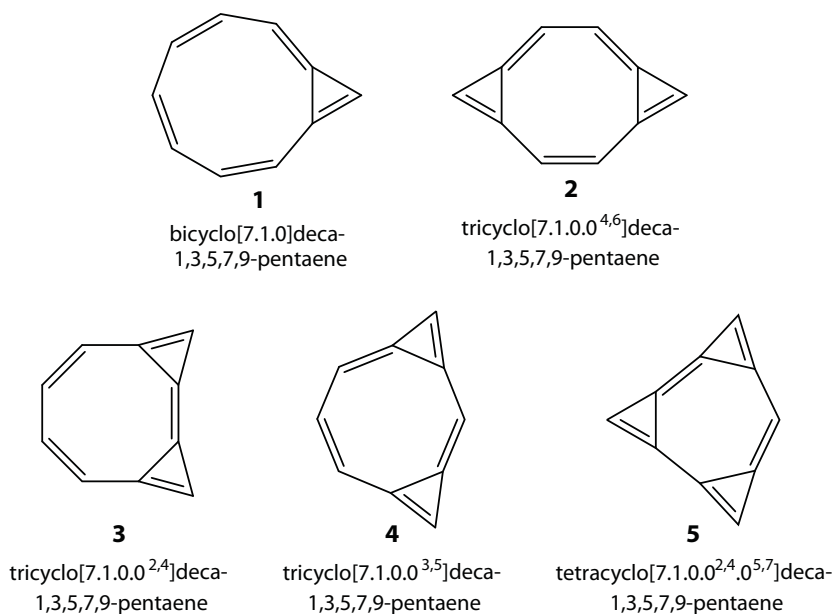


Figure 1: The ten- $\pi$ -electron bi-, tri- and tetracyclic fused aromatic compounds involving cyclopropenyl rings studied in this paper.

minimum through a calculation of analytical harmonic vibrational frequencies. All of these calculations were performed with GAUSSIAN09 [12], using the “VeryTight” convergence criteria in geometry optimizations. The optimized geometries are shown in Figure 2.

The calculations on azulene were carried out to validate MP2(Full)/cc-pVTZ as a level of theory that is appropriate for establishing the structural characteristics of aromatic systems containing fused odd-membered rings. We compared the MP2(Full)/cc-pVTZ optimized geometry and dipole moment of azulene to an experimental structure, determined from the microwave spectra of  $^{13}\text{C}$  and deuterium azulene isotopomers, and an experimental dipole moment, determined from Stark splittings, which were reported by Bauder *et al.* [13]. As can be seen in Figure 2, the carbon-carbon bond lengths in the MP2(Full)/cc-pVTZ and experimental geometries of azulene agree reasonably well (both geometries are of  $C_{2v}$  symmetry). The MP2(Full)/cc-pVTZ dipole moment at the experimental geometry was obtained as 0.94 D, in fair agreement with the experimental value of 0.8821(24) D [13]; the dipole moment computed at the MP2(Full)/cc-pVTZ optimized geometry, 0.93 D (see Table 1), turned out to be very slightly closer to the experimental value, and practically identical to an often quoted  $\pi$ -space multireference configuration interaction with single and double excitations (MR-SDCI) result reported by Grimme [14]. The lowest vibrational frequency of azulene obtained at the MP2(Full)/cc-pVTZ level,  $166\text{ cm}^{-1}$  (see Table 1), suggests that this level of theory is unlikely to be affected by the so-called “insidious two-electron intramolecular basis set incompleteness error”, which may cause popular quantum chemical methods, including MP2, in combination with certain basis sets, to erroneously predict that benzene and certain arenes are nonplanar [15] (see also the very recent research in that area reported in [16]).

Each of the lowest vibrational frequencies of azulene and compounds **1–5** shown in Table 1 is associated with an out-of-plane normal mode. The magnitudes of these frequencies suggest that the planar structures of **1** and **3** are more “flexible” than that of azulene with respect to out-of-plane distortions,

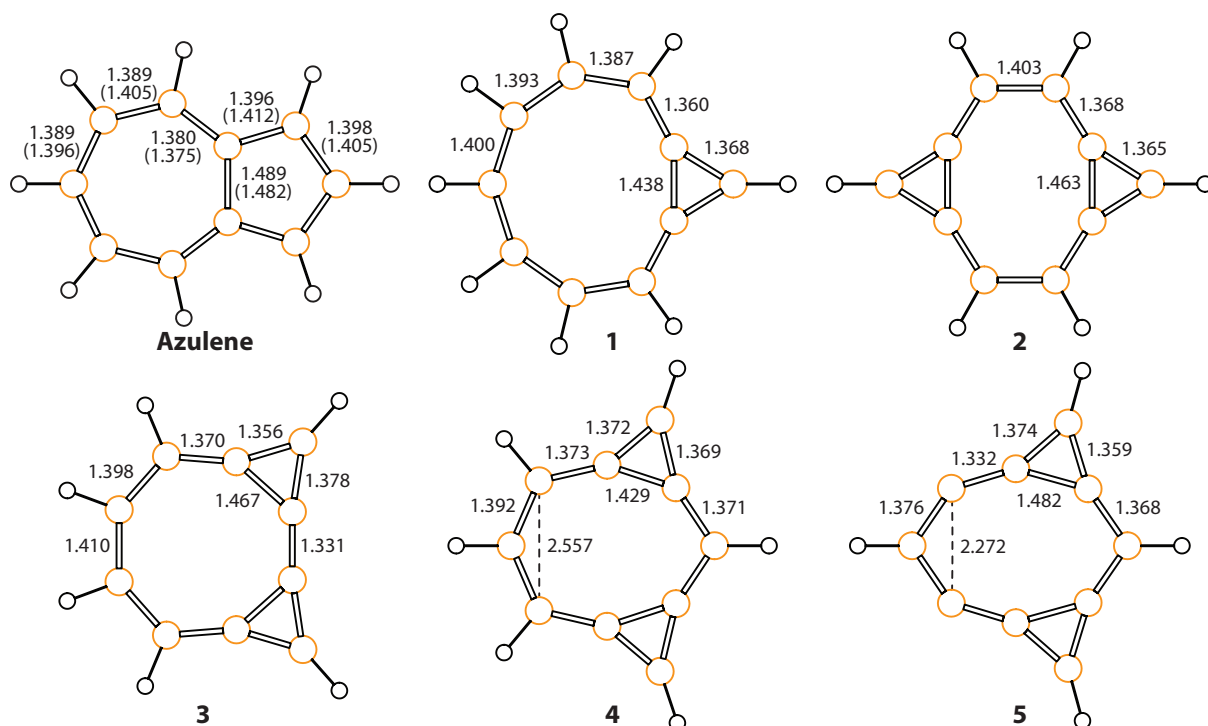


Figure 2: MP2(Full)/cc-pVTZ optimized ground state geometries of azulene and compounds **1**–**5** (azulene and **1**, **3**–**5**:  $C_{2v}$  symmetry; **2**:  $D_{2h}$  symmetry). Symmetry-unique bond lengths and other distances in Å; the experimental bond lengths in azulene [13] are given in brackets, rounded to three decimal places.

whereas those of **2**, **4** and, in particular, **5**, are more “rigid” with respect to such distortions.

Somewhat unexpectedly, the geometry optimization of **5** resulted in a tricyclic structure (see Figure 2) rather than the tetracyclic structure that was anticipated (see Figure 1). The tricyclic MP2(Full)/cc-pVTZ optimized geometry of **5** resembles a didehydro derivative of **4** akin to 1,3-didehydrobenzene (*m*-benzyne) [17], and it would be more appropriate to refer to it as 6,8-didehydro-tricyclo[7.1.0.0<sup>3,5</sup>]deca-1,3,5,7,9-pentaene. A plausible explanation for the tricyclic optimized geometry of **5** is that the  $\sigma$  and/or  $\pi$  bonding interactions between the dehydro centres are not sufficiently strong to overcome the ring strain that would be associated with the formation of a third three-membered ring; the presence of such bonding interactions between the dehydro centres is suggested by the fact that the distance between these centres is shorter than the distance between the corresponding carbon atoms in **4** (see Figure 2).

The MP2-level dipole moments ( $\mu_{\text{MP2}}$ ) of compounds **1** and **3**–**5**, reported in Table 1, are larger than might be expected from a visual comparison of their geometries to that of azulene (see Figure 2; due to its  $D_{2h}$  symmetry, **2** has no permanent dipole moment). As part of the SC analysis of the electronic structures of **1**–**5** (*vide infra*) we carried out  $\pi$ -space CASSCF(10,10)/cc-pVTZ calculations on these compounds at the respective MP2(Full)/cc-pVTZ optimized ground state geometries; such a calculation was also carried out for azulene. The CASSCF-level dipole moments ( $\mu_{\text{CASSCF}}$ ) obtained in these calculations are also shown in Table 1. All of the nonzero CASSCF-level dipole moments (for azulene, **1** and **3**–**5**) are smaller than the corresponding MP2-level values, with more pronounced differences being observed for azulene and for **1**. This is an indication that the inclusion of both dynamic and non-dynamic correlation effects could lower the MP2-level dipole moments of azulene, **1** and **3**–

Table 1: Lowest vibrational frequencies ( $\tilde{\nu}$ , in  $\text{cm}^{-1}$ , normal mode symmetries in brackets) for the MP2(Full)/cc-pVTZ optimized ground state geometries of azulene and compounds **1–5**, calculated at the MP2(Full)/cc-pVTZ level of theory, and MP2(Full) and CASSCF(10,10) dipole moments ( $\mu$ , in D) for the same geometry and basis set.

Compound	$\tilde{\nu}$	$\mu_{\text{MP2}}$	$\mu_{\text{CASSCF}}$
Azulene	166 ( $a_2$ )	0.93	0.69
<b>1</b>	128 ( $b_1$ )	2.27	1.85
<b>2</b>	170 ( $b_{3u}$ )	0.0	0.0
<b>3</b>	120 ( $a_2$ )	1.62	1.51
<b>4</b>	183 ( $b_1$ )	1.02	0.96
<b>5</b>	244 ( $b_1$ )	2.32	2.28

**5**, and perhaps improve the agreement between the theoretical and experimental values for the dipole moment of azulene; however, the theoretical estimates of the dipole moments of **1** and **3–5** are unlikely to decrease considerably. The CASSCF results were obtained both with GAUSSIAN09 [12] and MOLPRO [22, 23].

In order to describe the electronic structures of compounds **1–5**, we used  $\pi$ -space SC wavefunctions with ten singly-occupied non-orthogonal active  $\pi$  orbitals, SC(10), analogous to the one which was used for azulene in Ref. 3. A SC(10) wavefunction of this type can be written in the following form:

$$\Psi_{00}(10) = \hat{\mathcal{A}} \left[ \left( \prod_{i=1}^n \sigma_i \alpha \sigma_i \beta \right) \left( \prod_{\mu=1}^{10} \pi_{\mu} \right) \Theta_{00}^{10} \right] \quad (1)$$

where  $\sigma_i$  are the  $n$  doubly-occupied  $\sigma$  orbitals (the numbers of these orbitals for **1–5** are 29, 28, 28, 28, and 27, respectively); the “00” subscripts indicate the values of the total spin  $S$  and its  $z$ -projection  $M_S$  which, for a singlet state, are both equal to zero,  $S = M_S = 0$ ;  $\Theta_{00}^{10}$  denotes a general normalized ten-electron spin function, expanded in the full spin space [5] of 42 linearly-independent spin eigenfunctions  $\Theta_{00;k}^{10}$ ,

$$\Theta_{00}^{10} = \sum_{k=1}^{42} C_{0k} \Theta_{00;k}^{10} \quad (2)$$

Although the values of the spin-coupling coefficients,  $C_{0k}$ , depend on the spin basis that is used, the SC(10) wavefunction  $\Psi_{00}(10)$  is invariant to the choice of spin basis, provided that we include all 42 spin-coupling modes. In the present work, it proves most informative to use the Rumer basis [4] which is the one most closely associated with classical VB theory. Each of the 42 Rumer spin eigenfunctions for a ten-electron singlet,  ${}^R\Theta_{00;k}^{10}$ , can be uniquely identified by listing its five singlet-coupled pairs, as in the examples of  ${}^R\Theta_{00;1}^{10}$  and  ${}^R\Theta_{00;23}^{10}$  given below:

$$\begin{aligned} {}^R\Theta_{00;1}^{10} &= (1-2, 3-4, 5-6, 7-8, 9-10) \\ &= 2^{-5/2} [\alpha(1)\beta(2) - \alpha(2)\beta(1)] [\alpha(3)\beta(4) - \alpha(4)\beta(3)] \dots [\alpha(9)\beta(10) - \alpha(10)\beta(9)] \end{aligned} \quad (3)$$

and

$$\begin{aligned} {}^R\Theta_{00;23}^{10} &= (1 - 10, 2 - 3, 4 - 5, 6 - 7, 8 - 9) \\ &= 2^{-5/2}[\alpha(1)\beta(10) - \alpha(10)\beta(1)][\alpha(2)\beta(3) - \alpha(3)\beta(2)] \dots [\alpha(8)\beta(9) - \alpha(9)\beta(8)] \end{aligned} \quad (4)$$

In all of the SC(10) calculations we used the cc-pVTZ basis set and the geometries that had been optimized at the MP2(Full)/cc-pVTZ level of theory. As usual, the core and SC orbitals were approximated, as in molecular orbital (MO) theory, by linear expansions in the full cc-pVTZ basis set for the respective molecule. All of the orbital coefficients for active and inactive orbitals and the spin-coupling coefficients,  $C_{0k}$ , were determined variationally, by minimizing the energy expectation value of the SC(10) wavefunction using the CASVB algorithms [18–21] implemented in MOLPRO [22, 23].

Table 2: Total HF, SC(10) and CASSCF(10,10) energies of compounds **1–5** (in a.u.) and percentages of the CASSCF correlation energy that is recovered (in brackets).

Compound	Wavefunction	Total Energy
<b>1</b>	HF	−383.295 752 (0.0%)
	SC(10)	−383.397 135 (86.3%)
	CASSCF(10,10)	−383.413 220 (100.0%)
<b>2</b>	HF	−382.069 259 (0.0%)
	SC(10)	−382.171 159 (86.1%)
	CASSCF(10,10)	−382.187 628 (100.0%)
<b>3</b>	HF	−382.022 472 (0.0%)
	SC(10)	−382.129 020 (87.2%)
	CASSCF(10,10)	−382.144 726 (100.0%)
<b>4</b>	HF	−382.105 675 (0.0%)
	SC(10)	−382.183 873 (81.3%)
	CASSCF(10,10)	−382.201 902 (100.0%)
<b>5</b>	HF	−380.716 595 (0.0%)
	SC(10)	−380.804 272 (83.3%)
	CASSCF(10,10)	−380.821 826 (100.0%)

The total energies of the HF, SC(10) and CASSCF(10,10) wavefunctions for compounds **1–5**, and the percentages of CASSCF correlation energy accounted for by the SC(10) wavefunctions, are shown in Table 2. The SC(10) wavefunction includes just 42 non-orthogonal configuration state functions (CSFs) which correspond to combinations of the orbital product in Eq. (1) with each of the spin functions from Eq. (2). The CASSCF(10,10) wavefunction makes use of a significantly larger number of orthogonal CSFs, 19 404 in total. It is interesting to observe that the much more compact SC(10) wavefunction manages to recover high percentages (81.3%–87.2%) of the CASSCF(10,10) correlation energies for **1–5**, not far behind the 89.5% achieved by the SC(6) wavefunction for benzene (using five non-orthogonal CSFs, as opposed to the corresponding CASSCF(6,6) wavefunction with a total of 175 orthogonal CSFs, from calculations in the cc-pVTZ basis [2]).

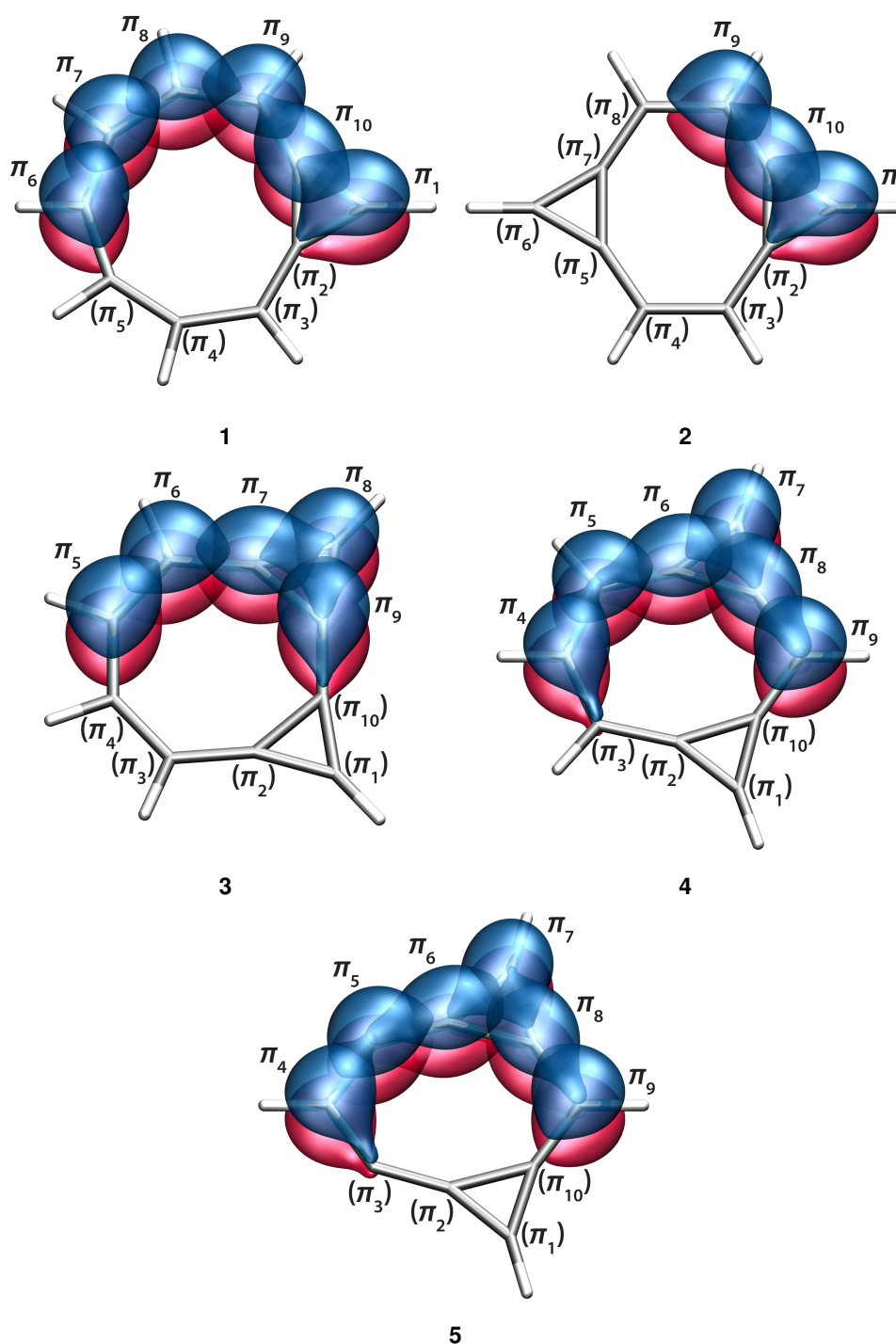


Figure 3: Symmetry-unique active orbitals from the SC(10) wavefunctions for **1–5**, represented as iso-value surfaces at  $\pi_\mu = \pm 0.1$ . The positions of the active orbitals which are not shown are indicated by orbital symbols in brackets. POV-Ray (Persistence of Vision Raytracer) files generated by VMD [24].

The symmetry-unique active orbitals from the SC(10) wavefunctions for compounds **1–5** are shown in Figure 3. All of these orbitals are reasonably similar in appearance and resemble distorted  $C(2p_\pi)$  atomic orbitals. Some of the relatively small variations in orbital shape are familiar from previous SC work. For example, the orbitals  $\pi_1$  on the outermost carbon atoms within the three-membered rings in **1–5** closely reproduce the active orbitals from the SC(2,3) (“two electrons in three orbitals”) wavefunction

for the cyclopropenium cation [25]; the orbitals that are outside three-membered rings look very much like the SC orbitals in benzene (see e.g. [2]). The impression created by the orbital shapes shown in Figure 3 is that the  $\pi$ -space SC orbitals form a “meccano set” with a small number of unique “parts” which can be neatly assembled to describe five different conjugated molecules.

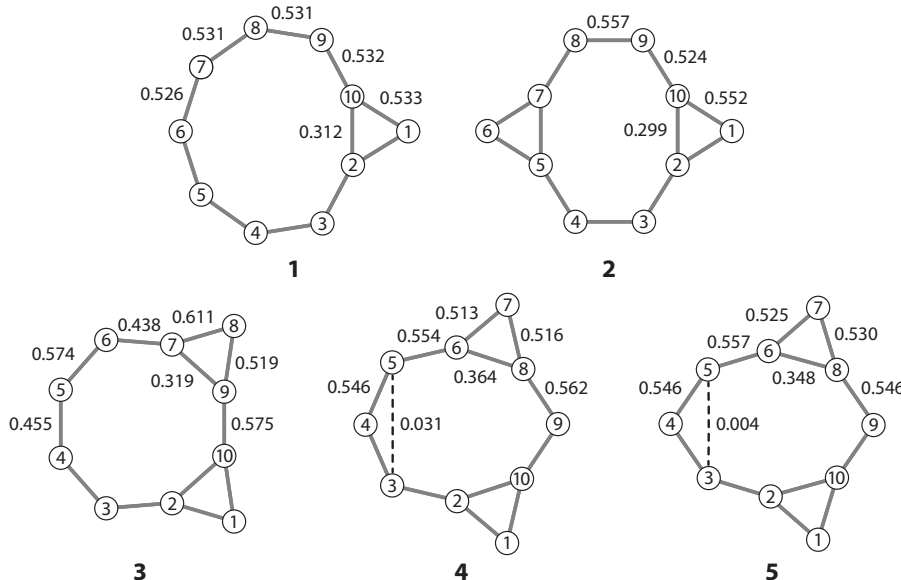


Figure 4: Symmetry-unique overlap integrals  $\langle \pi_\mu | \pi_{\mu+1} \rangle$  between adjacent SC orbitals for compounds **1–5**, and the  $\langle \pi_3 | \pi_5 \rangle$  overlap integrals for **4** and **5**.

The overlap integrals between SC orbitals associated with neighbouring carbon atoms are shown in Figure 4. For comparison, all overlap integrals between adjacent SC orbitals from the SC(6)/cc-pVTZ wavefunction for benzene are the same and equal to 0.525 [2]. Clearly, all  $\langle \pi_\mu | \pi_{\mu+1} \rangle$  overlap integrals along the outer perimeters of **1**, **2**, **4** and **5** are reasonably similar and close to the value obtained for benzene; the corresponding sequence of overlap integrals in **3** shows larger variations. Interestingly, the  $\langle \pi_8 | \pi_9 \rangle = 0.557$  and  $\langle \pi_9 | \pi_{10} \rangle = 0.524$  overlap integrals in **2** are over a longer and a shorter carbon-carbon bond of 1.403 and 1.368 Å, respectively (see Figure 2); a similar situation is observed in **3**, where the overlap integrals  $\langle \pi_5 | \pi_6 \rangle = 0.574$  and  $\langle \pi_6 | \pi_7 \rangle = 0.438$  are over carbon-carbon bonds of 1.398 and 1.370 Å. In both cases, one of the orbitals in the smaller overlap integral ( $\pi_{10}$  in **2** and  $\pi_7$  in **3**) has a large overlap with another orbital ( $\pi_1$  in **2** and  $\pi_8$  in **3**); the ensuing changes in orbital shapes are responsible for the observed disparities between the associated overlap integrals and the corresponding carbon-carbon bond lengths. The decrease in the  $\langle \pi_3 | \pi_5 \rangle$  overlap on passing from **4** to **5** suggests that the contribution of SC orbitals  $\pi_3$  and  $\pi_5$  to the bonding interactions between the dehydro centres in **5** is negligible.

The relative importance of the 42 ten-electron singlet Rumer spin functions participating in the SC(10) wavefunctions for compounds **1–5** was analysed by calculating their Chirgwin-Coulson weights [26] within the normalized active-space spin functions from Eq. (2). In all cases it turned out that the two most important Rumer spin functions are the “Kekulé” spin functions  $\Theta_{K_1}^{10} = {}^R\Theta_{00;1}^{10}$  and  $\Theta_{K_2}^{10} = {}^R\Theta_{00;23}^{10}$  [see Eqs. (3) and (4)].

In the lowest-energy SC(10) wavefunctions for **1–5**, corresponding to the respective singlet electronic ground states ( $S_0$ ), the spin-coupling coefficients for the two “Kekulé” spin functions  $C_{K_1} = C_{01}$



and  $C_{K_2} = C_{0,23}$  (see Eq. (2)) have the same sign, which indicates the presence in each of these wavefunctions of the SC analogue of the classical VB resonance between two Kekulé structures. The resonance patterns in **1–5** and the Chirgwin-Coulson weights of  $\Theta_{K_1}^{10}$  and  $\Theta_{K_2}^{10}$  are shown in Figure 5. The two “Kekulé” spin functions are equivalent by symmetry in all compounds except **3**; these two spin functions account for 65.8%, 62.1%, 57.8%, 98.9% and 84.1% of the ground state spin functions of **1**, **2**, **3**, **4** and **5**, respectively. The weights of the next most important Rumer spin functions in the  $S_0$  active-space spin functions of **1–5** are much smaller, 4.9%, 9.0%, 6.6%, 5.8% and 6.4%, respectively (note that although the Chirgwin-Coulson weights add to 100%, some of these can be negative, due to the non-orthogonality of the Rumer spin functions). The resonance patterns observed in the SC(10) wavefunctions for the singlet electronic ground states of **1–5** suggest that all of these fused-ring planar conjugated systems are aromatic.

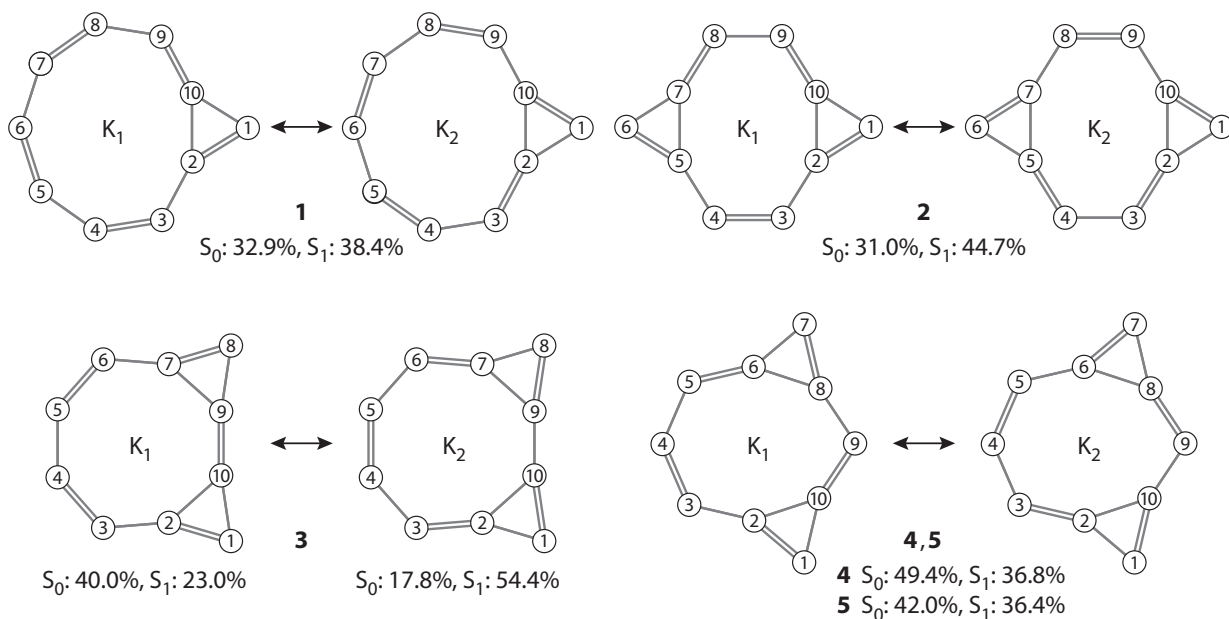


Figure 5: SC resonance patterns for compounds **1–5** showing the dominant “Kekulé” spin functions  $\Theta_{K_1}^{10} = {}^R\Theta_{00;1}^{10}$  and  $\Theta_{K_2}^{10} = {}^R\Theta_{00;23}^{10}$  and their weights in the electronic ground states  $S_0$  and first singlet excited states  $S_1$ .

The large Chirgwin-Coulson weights of  $\Theta_{K_1}^{10}$  and  $\Theta_{K_2}^{10}$  suggest that the SC(10) wavefunctions for compounds **1–5** (see Eq. (1)) could be approximated by retaining just these two spin functions and omitting the remaining 40 Rumer spin functions:

$$\Psi_{00}(10) \approx \Psi'_{00}(10) = \hat{\mathcal{A}} \left[ \left( \prod_{i=1}^n \sigma_i \alpha \sigma_i \beta \right) \left( \prod_{\mu=1}^{10} \pi_{\mu} \right) \left( C_{K_1} \Theta_{K_1}^{10} + C_{K_2} \Theta_{K_2}^{10} \right) \right] \quad (5)$$

We fully optimized the very compact  $\Psi'_{00}(10)$  wavefunctions for **1–5** and established that these wavefunctions still recover 82.5%, 81.8%, 82.5%, 79.4% and 80.5%, respectively, of the corresponding CASSCF(10,10) correlation energies given in Table 2. These percentages are only 1.8–4.7% lower than the corresponding values that were obtained with the complete SC(10) wavefunctions (see Table 2) and confirm the importance of the “Kekulé” spin functions for understanding the electronic structures of

**1–5.** As expected from the results of the complete SC(10) calculations, the optimized spin-coupling coefficients  $C_{K_1}$  and  $C_{K_2}$  turned out to be of the same sign in all of the  $\Psi'_{00}(10)$  wavefunctions.

If we treat the SC(10) wavefunction in Eq. (1) as a linear combination of 42 non-orthogonal CSFs, then the lowest root of the secular problem in terms of these CSFs will, of course, correspond to the electronic ground state  $S_0$ , while the next root will provide an approximation to the first singlet excited state  $S_1$ , utilizing the same orbitals, but with different spin-coupling coefficients. The analysis of the spin-coupling coefficients defining these approximations to the  $S_1$  states of **1–5** shows that the corresponding active-space spin functions are still dominated by the two “Kekulé” spin functions  $\Theta_{K_1}^{10}$  and  $\Theta_{K_2}^{10}$  except that, this time,  $\Theta_{K_1}^{10}$  and  $\Theta_{K_2}^{10}$  are in “antiresonance”: the spin-coupling coefficients  $C_{K_1}$  and  $C_{K_2}$  are of opposite signs. Assuming positive  $C_{K_1}$  and  $C_{K_2}$ , the approximate  $S_1$  wavefunctions for **1–5** can be expressed as

$$\Psi_{00}(10, S_1) \approx \hat{\mathcal{A}} \left[ \left( \prod_{i=1}^n \sigma_i \alpha \sigma_i \beta \right) \left( \prod_{\mu=1}^{10} \pi_\mu \right) \left( C_{K_1} \Theta_{K_1}^{10} - C_{K_2} \Theta_{K_2}^{10} \right) \right] \quad (6)$$

The Chirgwin-Coulson weights of  $\Theta_{K_1}^{10}$  and  $\Theta_{K_2}^{10}$  in the  $S_1$  states of **1–5** are shown in Figure 5 alongside the corresponding numbers for the  $S_0$  states.

It has been shown using non-orthogonal configuration interaction constructions on top of a SC(6) reference that the  $S_1$  state of benzene is dominated by an out-of-phase combination of the two well-known Kekulé structures [27], whereas  $S_0$  is well approximated by an in-phase combination of these structures [28]. There is a growing body of theoretical evidence which strongly suggests that benzene switches from aromatic to antiaromatic on passing from  $S_0$  to  $S_1$  (see e.g. [29–31]). Given that the main difference between the modern VB descriptions of the  $S_0$  and  $S_1$  states of benzene is in the “resonance” or “antiresonance” involving the two Kekulé structures, it is reasonable to suppose that other cyclic conjugated systems exhibiting similar characteristics in their  $S_0$  and  $S_1$  states, would behave in the same manner. On this basis, it could be expected that compounds **1–5** become antiaromatic in their first singlet excited states.

The very low overlap integral between SC orbitals  $\pi_3$  and  $\pi_5$  in compound **5** (*vide supra*) is an indication that any bonding interaction between the dehydro centres is likely to be predominantly  $\sigma$  in character. In order to investigate this interaction in greater detail, we carried out an additional SC(12)/cc-pVTZ calculation on **5**, expanding the active space with two  $\sigma$  orbitals,  $\sigma'$  and  $\sigma''$ , and reducing, by one, the number of the doubly-occupied  $\sigma$  orbitals. The SC(12) wavefunction for **5** can be written down as

$$\Psi_{00}(12) = \hat{\mathcal{A}} \left[ \left( \prod_{i=1}^{26} \sigma_i \alpha \sigma_i \beta \right) \left( \prod_{\mu=1}^{10} \pi_\mu \right) \sigma' \sigma'' \Theta_{00}^{12} \right] \quad (7)$$

where the twelve-electron active-space spin function  $\Theta_{00}^{12}$  is defined analogously to  $\Theta_{00}^{10}$  in Eq. (2), but the expansion takes place over the full spin space of 132 linearly-independent twelve-electron singlet spin eigefunctions. Just as in the case of the SC(10)/cc-pVTZ calculations on **1–5**, all orbital and spin-coupling coefficients in this SC(12) wavefunction were determined variationally, using the CASVB algorithms in MOLPRO. The ten  $\pi$  SC orbitals  $\pi_1$ – $\pi_{10}$  turned out to be almost indistinguishable from those included in Figure 3. The two  $\sigma$  SC orbitals  $\sigma'$  and  $\sigma''$  are shown in Figure 6.  $\sigma'$  and  $\sigma''$  resemble distorted carbon  $sp^2$  hybrid orbitals pointing outside the seven-membered ring; carbon-based SC orbitals of a very similar shape have been observed in SC studies of *o*-benzyne [32] and *p*-benzyne (see [33] and its supporting information). The spins of SC orbitals  $\sigma'$  and  $\sigma''$  are predominantly singlet-coupled, and

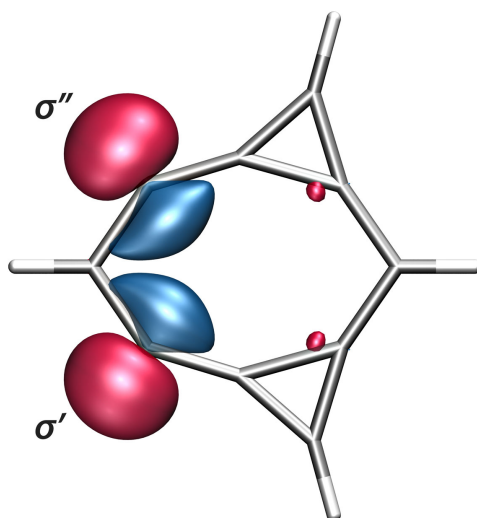


Figure 6: SC orbitals  $\sigma'$  and  $\sigma''$  from the SC(12) wavefunction for **5**. Details as for Fig. 3.

the relatively low value of the overlap integral  $\langle \sigma' | \sigma'' \rangle = 0.152$  suggest that these orbitals are responsible for only a weak  $\sigma$  bonding interaction between the dehydro centres in **5**.

### 3 Conclusions

Three quantum-chemical approaches, namely MP2, SC and CASSCF, in conjunction with the cc-pVTZ basis, were used to explore the ground state geometries and electronic structures of five ten- $\pi$ -electron bi-, tri- and tetracyclic fused conjugated molecules involving cyclopropenyl rings: bicyclo[7.1.0]deca-1,3,5,7,9-pentaene, tricyclo[7.1.0.0<sup>4,6</sup>]deca-1,3,5,7,9-pentaene, tricyclo[7.1.0.0<sup>2,4</sup>]deca-1,3,5,7,9-pentaene, tricyclo[7.1.0.0<sup>3,5</sup>]deca-1,3,5,7,9-pentaene and tetracyclo[7.1.0.0<sup>2,4</sup>.0<sup>5,7</sup>]deca-1,3,5,7,9-pentaene (see **1–5** in Figure 1). The results of the MP2(Full)/cc-pVTZ geometry optimizations and analytical harmonic vibrational frequency calculations show that all of these compounds can be expected to have stable planar ground state geometries of either  $C_{2v}$  or  $D_{2h}$  symmetry (see Figure 2). The geometry optimization of tetracyclo[7.1.0.0<sup>2,4</sup>.0<sup>5,7</sup>]deca-1,3,5,7,9-pentaene did not produce the expected tetracyclic structure; instead, the result was a tricyclic structure, 6,8-didehydro-tricyclo[7.1.0.0<sup>3,5</sup>]deca-1,3,5,7,9-pentaene, which can be viewed as a dehydro derivative of tricyclo[7.1.0.0<sup>3,5</sup>]deca-1,3,5,7,9-pentaene, similar to 1,3-didehydrobenzene (*m*-benzyne). According to the results of the MP2(Full)/cc-pVTZ and CASSCF(10,10)/cc-pVTZ calculations, all compounds with ground state geometries of  $C_{2v}$  symmetry are predicted to have high dipole moments (see Table 1).

SC wavefunctions with ten active  $\pi$  orbitals, SC(10)/cc-pVTZ, were used to obtain modern VB descriptions of the ground state electronic structures of all five of the fused conjugated molecules. An additional larger SC(12)/cc-pVTZ calculation with ten active  $\pi$  and two active  $\sigma$  orbitals was carried out for 6,8-didehydro-tricyclo[7.1.0.0<sup>3,5</sup>]deca-1,3,5,7,9-pentaene in order to examine the presence and extent of  $\sigma$  bonding between the dehydro centres. Using just 42 non-orthogonal CSFs, the SC(10) wavefunctions described in this paper were found to capture 81.3%–87.2% of the correlation energies included in their CASSCF(10,10) counterparts, each of which comprises a total of 19 404 orthogonal CSFs. This is an indication that these SC(10) wavefunctions carry most of the essential electronic struc-

ture information contained in the corresponding CASSCF(10,10) constructions but are more compact and much easier to interpret. As in previous SC studies of conjugated systems, all of the active  $\pi$  orbitals for each of these fused conjugated molecules came out as atom-centred, well-localized and similar in appearance to  $C(2p_\pi)$  atomic orbitals with small symmetrical protrusions towards neighbouring carbon atoms. A comparison between the shapes of the active  $\pi$  orbitals for the conjugated systems studied in this paper and those for other planar conjugated systems, in particular, aromatic annulene ions [25], shows levels of similarity which suggest that such orbitals, when placed in matching environments, are largely transferable between systems.

The active-space spin function within the ground state SC(10) wavefunction for each of the five fused conjugated molecules examined in this paper was found to be dominated by two “Kekulé” Rumer spin functions; the coefficients for these spin functions have the same sign and suggest the establishment of the well-known classical VB resonance picture associated with aromatic behaviour. However, within the SC(10) approximation for the wavefunction of the first singlet excited state of each of these five fused conjugated molecules, which still involves two dominant “Kekulé” Rumer spin functions, the coefficients for these spin functions turned out to have opposite signs. In this way, the resonance observed in the electronic ground states of the five fused conjugated molecules appears to be replaced by “antiresonance” in the respective first singlet excited states, suggesting that all of these excited states are antiaromatic. Of course, these considerations apply to vertical excitations only; if the excited state geometries are allowed to relax, they are likely to adopt instead conformations in which the levels of antiaromaticity are considerably reduced.

## References

- [1] D.L. Cooper, P.B. Karadakov, Spin-Coupled Descriptions of Organic Reactivity, *Int. Rev. Phys. Chem.*, 28 (2009) 169–206.
- [2] P.B. Karadakov, D.L. Cooper, B.J. Duke, J. Li, Spin-Coupled Theory for ‘ $N$  Electrons in  $M$  Orbitals’ Active Spaces, *J. Phys. Chem. A*, 116 (2012) 7238–7244.
- [3] G. Raos, J. Gerratt, D.L. Cooper, M. Raimondi, Spin Correlation in  $\pi$ -Electron Systems from Spin-Coupled Wavefunctions. II. Further Applications, *Chem. Phys.*, 186 (1994) 251–273.
- [4] G. Rumer, Zur Theorie der Spinvalenz, *Göttinger Nachr.*, 3 (1932) 337–341.
- [5] R. Pauncz, Spin Eigenfunctions. Construction and Use, Plenum Press, New York and London, 1979, p17.
- [6] T.M. Cresp, F. Sondheimer, The Synthesis of Derivatives of [14]Annuleno[14]annulene, [14]Annuleno[16]annulene, and [14]Annuleno[18]annulene, Bicyclic Compounds Consisting of Two Ortho Fused Macrocyclic Conjugated  $\pi$  Systems, *J. Am. Chem. Soc.*, 99 (1977) 194–204.
- [7] A. Toyota, T. Nakajima, Molecular-Symmetry Reduction in  $C_mH_{m-2}$  Cata-Condensed Nonalternant Hydrocarbons, *Bull. Chem. Soc. Jpn.*, 46 (1973) 3681–3685.
- [8] I. Agranat, B.A. Hess, Jr., L.J. Schaad, Aromaticity of Non-Alternant Annulenoannulenes and of Corannulenes, *Pure & Appl. Chem.* 52 (1980) 1399–1407.

- [9] R.W.A. Havenith, F. Lugli, P.W. Fowler, E. Steiner, Ring Current Patterns in Annelated Bicyclic Polyenes, *J. Phys. Chem. A* 106 (2002) 5703–5708.
- [10] A. Muñoz-Castro, On the Fused-to-Single Ring Transition in  $10\pi$  Structures. Insights from Naphthalene to [10]Annulene Series, *Chem. Phys. Lett.* 650 (2016) 60–63.
- [11] A. Toyota, On the Stable Molecular-Shapes of  $C_mH_{m-4}$  Cata-Condensed Nonalternant Hydrocarbons, *Bull. Chem. Soc. Jpn.*, 48 (1975) 1152–1156.
- [12] M.J. Frisch, G.W. Trucks, H.B. Schlegel, G.E. Scuseria, M.A. Robb, J.R. Cheeseman, G. Scalmani, V. Barone, B. Mennucci, G.A. Petersson, H. Nakatsuji, M. Caricato, X. Li, H.P. Hratchian, A.F. Izmaylov, J. Bloino, G. Zheng, J.L. Sonnenberg, M. Hada, M. Ehara, K. Toyota, R. Fukuda, J. Hasegawa, M. Ishida, T. Nakajima, Y. Honda, O. Kitao, H. Nakai, T. Vreven, J.A. Montgomery Jr., J.E. Peralta, F. Ogliaro, M. Bearpark, J.J. Heyd, E. Brothers, K.N. Kudin, V.N. Staroverov, R. Kobayashi, J. Normand, K. Raghavachari, A. Rendell, J.C. Burant, S.S. Iyengar, J. Tomasi, M. Cossi, N. Rega, J.M. Millam, M. Klene, J.E. Knox, J.B. Cross, V. Bakken, C. Adamo, J. Jaramillo, R. Gomperts, R.E. Stratmann, O. Yazyev, A.J. Austin, R. Cammi, C. Pomelli, J.W. Ochterski, R.L. Martin, K. Morokuma, V.G. Zakrzewski, G.A. Voth, P. Salvador, J.J. Dannenberg, S. Dapprich, A.D. Daniels, Ö. Farkas, J.B. Foresman, J.V. Ortiz, J. Cioslowski, D.J. Fox, Gaussian 09, Revision D.01, Gaussian, Inc., Wallingford, CT, 2009.
- [13] S. Huber, G. Grassi, A. Bauder, Structure and Symmetry of Azulene as Determined from Microwave Spectra of Isotopomers, *Mol. Phys.*, 103 (2005) 1395–1409.
- [14] S. Grimme, Ab Initio Study of the Structure and Dipole Moment of Azulene, *Chem. Phys. Lett.* 201 (1993) 67–74.
- [15] D. Moran, A.C. Simmonett, F.E. Leach III, W.D. Allen, P.v.R. Schleyer, H.F. Schaefer III, Popular Theoretical Methods Predict Benzene and Arenes to Be Nonplanar, *J. Am. Chem. Soc.*, 128 (2006) 9342–9343.
- [16] P.B. Karadakov, Do Large Polycyclic Aromatic Hydrocarbons and Graphene Bend? How Popular Theoretical Methods Complicate Finding the Answer to This Question. *Chem. Phys. Lett.*, 646 (2016) 190–196.
- [17] R. Marquardt, W. Sander, E. Kraka, 1,3-Didehydrobenzene (*m*-Benzyne), *Angew. Chem. Int. Ed. Engl.*, 35 (1996) 746–747.
- [18] T. Thorsteinsson, D.L. Cooper, J. Gerratt, P.B. Karadakov, M. Raimondi, Modern Valence Bond Representations of CASSCF Wavefunctions, *Theor. Chim. Acta*, 93 (1996) 343–366.
- [19] D.L. Cooper, T. Thorsteinsson, J. Gerratt, Modern VB Representations of CASSCF Wave Functions and the Fully-Variational Optimization of Modern VB Wave Functions Using the CASVB Strategy, *Adv. Quant. Chem.*, 32 (1998) 51–67.
- [20] T. Thorsteinsson, D.L. Cooper, Nonorthogonal Weights of Modern VB Wave Functions. Implementation and Applications within CASVB, *J. Math. Chem.*, 23 (1998) 105–126.

- [21] T. Thorsteinsson, D.L. Cooper, An Overview of the CASVB Approach to Modern Valence Bond Calculations, in: A. Hernández-Laguna, J. Maruani, R. McWeeny, S. Wilson (Eds.) *Quantum Systems in Chemistry and Physics. Volume 1: Basic Problems and Model Systems*, Kluwer, Dordrecht, 2000, pp. 303–326.
- [22] H.-J. Werner, P.J. Knowles, G. Knizia, F.R. Manby, M. Schütz, Molpro: A General-Purpose Quantum Chemistry Program Package, *WIREs Comput. Mol. Sci.*, 2 (2012) 242–253.
- [23] MOLPRO, Version 2015.1, A Package of Ab Initio Programs, H.-J. Werner, P.J. Knowles, G. Knizia, F.R. Manby, M. Schütz, P. Celani, W. Györfy, D. Kats, T. Korona, R. Lindh, A. Mitrushenkov, G. Rauhut, K. R. Shamasundar, T. B. Adler, R. D. Amos, A. Bernhardsson, A. Berning, D. L. Cooper, M. J. O. Deegan, A. J. Dobbyn, F. Eckert, E. Goll, C. Hampel, A. Hesselmann, G. Hetzer, T. Hrenar, G. Jansen, C. Köppl, Y. Liu, A. W. Lloyd, R. A. Mata, A. J. May, S. J. McNicholas, W. Meyer, M. E. Mura, A. Nicklaß, D. P. O'Neill, P. Palmieri, D. Peng, K. Pflüger, R. Pitzer, M. Reiher, T. Shiozaki, H. Stoll, A. J. Stone, R. Tarroni, T. Thorsteinsson, M. Wang, see <http://www.molpro.net>.
- [24] W. Humphrey, A. Dalke, K. Schulten, VMD—Visual Molecular Dynamics, *J. Molec. Graphics*, 14 (1996) 33–38, see <http://www.ks.uiuc.edu/Research/vmd/>.
- [25] P.B. Karadakov, D.L. Cooper, Modern Valence-Bond Description of Aromatic Annulene Ions, *Theor. Chem. Acc.*, 133 (2014) 1421–1429.
- [26] B.H. Chirgwin, C.A. Coulson, The Electronic Structure of Conjugated Systems. VI. *Proc. Roy. Soc. Lond. Ser. A*, 201 (1950) 196–209.
- [27] E.C. da Silva, J. Gerratt, D.L. Cooper, M. Raimondi, Study of the Electronic States of the Benzene Molecule using Spin-Coupled Valence Bond Theory, *J. Chem. Phys.*, 101 (1994) 3866–3887.
- [28] D.L. Cooper, J. Gerratt, M. Raimondi, The Electronic Structure of the Benzene Molecule, *Nature*, 323 (1986) 699–701.
- [29] P.B. Karadakov, Ground and Excited State Aromaticity and Antiaromaticity in Benzene and Cyclobutadiene, *J. Phys. Chem. A*, 112 (2008) 7303–7309.
- [30] F. Feixas, J. Vandenbussche, P. Bultinck, E. Matitoc, M. Solà, Electron Delocalization and Aromaticity in Low-Lying Excited States of Archetypal Organic Compounds, *Phys. Chem. Chem. Phys.*, 13 (2011) 20690–20703.
- [31] P. B. Karadakov, P. Hearnshaw and K.E. Horner, Magnetic Shielding, Aromaticity, Antiaromaticity and Bonding in the Low-Lying Electronic States of Benzene and Cyclobutadiene, *J. Org. Chem.* (2016), DOI: 10.1021/acs.joc.6b02460.
- [32] P.B. Karadakov, J. Gerratt, G. Raos, D.L. Cooper, M. Raimondi, The Lowest Singlet and Triplet States of *o*-Benzyne: Spin-Coupled Interpretation of the Electronic Structure at CASSCF Equilibrium Geometries, *Isr. J. Chem.*, 33 (1993) 253–264.
- [33] D.L. Cooper, P.B. Karadakov, B.J. Duke, Bonding in Singlet and Triplet Butalene: Insights from Spin-coupled Theory, *J. Phys. Chem. A*, 119 (2015) 2169–2175.